ADP-10-25/T721

Roper Resonance in 2+1 Flavor QCD

M. Selim Mahbub,[1,2] Waseem Kamleh,[1] Derek B. Leinweber,[1] Peter J. Moran,[1,3] and Anthony G. Williams[1]
(CSSM Lattice Collaboration)
[1]*Special Research Centre for the Subatomic Structure of Matter, Adelaide, South Australia 5005, Australia, and Department of Physics, University of Adelaide, South Australia 5005, Australia.*
[2]*Department of Physics, Rajshahi University, Rajshahi 6205, Bangladesh.*
[3]*CSIRO Mathematics, Informatics and Statistics, Private Bag 33, Clayton South, VIC 3169, Australia.*

The low-lying even-parity states of the nucleon are explored in lattice QCD using the PACS-CS collaboration 2+1-flavor dynamical-QCD gauge-field configurations made available through the International Lattice Datagrid (ILDG). The established correlation-matrix approach is used, in which various fermion source and sink smearings are utilized to provide an effective basis of interpolating fields to span the space of low-lying energy eigenstates. Of particular interest is the nature of the first excited state of the nucleon, the $N\frac{1}{2}^+$ Roper resonance of P_{11} pion-nucleon scattering. The Roper state of the present analysis approaches the physical mass, displaying significant chiral curvature at the lightest quark mass. These full QCD results, providing the world's first insight into the nucleon mass spectrum in the light-quark regime, are significantly different from those of quenched QCD and provide interesting insights into the dynamics of QCD.

PACS numbers: 11.15.Ha,12.38.Gc,12.38.-t

The first positive parity resonance of the nucleon, the $N\frac{1}{2}^+(1440)$ or Roper resonance, has been a subject of extensive interest since its discovery in 1964 [1]. This P-wave isospin-1/2 spin-1/2 (P_{11}) pion-nucleon resonance has held the curiosity and imagination of the nuclear and particle physics community due to its surprisingly low mass. For example, in constituent quark models the lowest-lying odd-parity state occurs below the P_{11} state [2, 3] whereas in Nature, the negative parity $N\frac{1}{2}^-(1535)$ S_{11} state is almost 100 MeV *above* the Roper resonance.

This phenomenon has led to wide speculation on the possible exotic nature of the Roper resonance. For example, the Roper resonance has been described as a hybrid baryon state with explicitly excited gluon field configurations [4, 5], as a breathing mode of the ground state [6] or a state which can be described in terms of a five quark (meson-baryon) state [7].

The elusive nature of this low-lying resonance is not constrained to model calculations alone. There have been several investigations of the low-lying nucleon spectrum using the first-principles approach of lattice field theory.

The lattice approach to Quantum Chromodynamics (QCD) provides a non-perturbative tool to explore the properties of hadrons from the first principles of this fundamental quantum field theory. Numerical simulations of QCD on a space-time lattice with the light up, down and strange dynamical-quark masses similar to those of Nature are now possible [8]. As such, some long-standing problems in nuclear-particle physics are now being resolved. For example, the ground-state hadron spectrum is now well understood [9].

However, gaining knowledge of the excited-state spectrum presents additional challenges. The Euclidean-time correlation function provides access to a tower of energy eigenstates in the form of a sum of decaying exponentials with the masses of the states in the exponents. The ground state mass, being the lowest energy state, has the slowest decay rate, and is obtained through the analysis of the large-time behaviour of this function. However, the excited states appear in the the sub-leading exponentials. Extracting excited state masses from these exponents is intricate as the correlation functions decay quickly and the signal to noise ratio deteriorates rapidly. In addition, the spectrum is composed of both single-particle states and multiple-particle states interacting and mixing in the finite physical volume of the lattice. Understanding the finite-volume dependence of these states and linking them to the resonances of Nature is a long-term program of the lattice QCD community.

In this letter we report the excited-state energy spectrum of the nucleon in the light quark-mass regime of QCD for the first time. Of particular note is the identification of a new low-lying state associated with the Roper resonance of Nature.

Several attempts have been made in the past to find the elusive low-lying Roper state in the lattice framework [10–15, 15–22]. The results reported therein are as much about the development of lattice techniques as they are about the nucleon spectrum. Where the lattice techniques are regarded as robust, a low-lying Roper state has not been observed. The difficulties lie in finding effective methods to isolate the energy eigenstates of QCD and in accessing the light quark mass regime of QCD.

The 'Variational method' [23, 24] is the state-of-the-art approach for determining the excited state hadron spectrum. It is based on the creation of a matrix of correlation functions in which different superpositions of excited state contributions are linearly combined to isolate the energy eigenstates. A diversity of excited-state superpositions is central to the success of this method.

Early implementations of this method using a variety of standard spin-flavor interpolating fields of fixed source-distribution size were not successful in isolating energy eigenstates. Instead the putative eigenstates were superpositions of energy-states [25] and the low-lying Roper state was hidden by excited-state contaminations. A solution to this problem was established in Refs. [26, 27] where a low-lying Roper state was isolated. Key to this approach, used herein, is the utilization of a diverse range of fermion source and sink smearings in creating the matrix of correlation functions. The diversity of smearings leads to a wide variety of superpositions of excited-state contributions, providing a suitable basis for constructing linear combinations which isolate the eigenstates.

These effective techniques [25–28] were developed in the quenched approximation and we bring them to the dynamics of full QCD for the first time here. The low-lying even-parity states of the nucleon are explored in full QCD using 2+1-flavor dynamical-QCD gauge-field configurations [8]. Whereas other recent full QCD analyses [20–22] report a first positive parity excited state that appears too high to be considered as the Roper resonance, we will illustrate how the low-lying Roper state of the present analysis approaches the physical mass of Nature, displaying significant chiral curvature at the lightest quark mass (corresponding to a pion mass of 160 MeV, only slightly above the physical value of 140 MeV). These full QCD results, providing the world's first insight into the nucleon mass spectrum in the light-quark regime, are significantly different from those of quenched QCD and provide interesting insights into the dynamics of QCD.

In constructing our correlation matrix for the nucleon spectrum, we consider the two-point correlation function matrix with momentum $\vec{p} = 0$

$$G^{\pm}_{ij}(t) = \sum_{\vec{x}} \mathrm{Tr}_{\mathrm{sp}} \{\Gamma_{\pm} \langle\Omega|\chi_i(x)\,\bar{\chi}_j(0)|\Omega\rangle\}, \quad (1)$$

$$= \sum_{\alpha} \lambda^{\alpha}_i\,\bar{\lambda}^{\alpha}_j\,e^{-m_{\alpha} t}, \quad (2)$$

where Dirac indices are implicit. Here, λ^{α}_i and $\bar{\lambda}^{\alpha}_j$ are the couplings of the interpolators χ_i and $\bar{\chi}_j$ at the sink and source respectively and α enumerates the energy eigenstates with mass m_{α}. $\Gamma_{\pm} = \frac{1}{2}(\gamma_0 \pm 1)$ projects the parity of the eigenstates.

Since the only t dependence comes from the exponential term, one can seek a linear superposition of interpolators, $\bar{\chi}_j u^{\alpha}_j$, such that

$$G_{ij}(t_0 + \triangle t)\,u^{\alpha}_j = e^{-m_{\alpha}\triangle t}\,G_{ij}(t_0)\,u^{\alpha}_j, \quad (3)$$

for sufficiently large t_0 and $t_0 + \triangle t$. Multiplying the above equation by $[G_{ij}(t_0)]^{-1}$ from the left leads to an eigenvalue equation

$$[(G(t_0))^{-1}\,G(t_0 + \triangle t)]_{ij}\,u^{\alpha}_j = c^{\alpha}\,u^{\alpha}_i, \quad (4)$$

where $c^{\alpha} = e^{-m_{\alpha}\triangle t}$ is the eigenvalue. Similar to Eq. (4), one can also solve the left eigenvalue equation to recover the v^{α} eigenvector

$$v^{\alpha}_i\,[G(t_0 + \triangle t)\,(G(t_0))^{-1}]_{ij} = c^{\alpha}\,v^{\alpha}_j. \quad (5)$$

The vectors u^{α}_j and v^{α}_i diagonalize the correlation matrix at time t_0 and $t_0 + \triangle t$ and provide the projected correlator

$$v^{\alpha}_i\,G^{\pm}_{ij}(t)\,u^{\beta}_j \propto \delta^{\alpha\beta}. \quad (6)$$

The parity projected, eigenstate projected correlator

$$G^{\alpha}_{\pm} \equiv v^{\alpha}_i\,G^{\pm}_{ij}(t)\,u^{\alpha}_j, \quad (7)$$

is then analyzed using standard techniques to obtain the masses of different states [14, 25, 29].

The PACS-CS $2+1$ flavor dynamical-fermion configurations [8] made available through the ILDG are used herein. These configurations use the non-perturbatively $\mathcal{O}(a)$-improved Wilson fermion action and the Iwasaki-gauge action [30]. The lattice volume is $32^3 \times 64$, with $\beta = 1.90$ providing a lattice spacing $a = 0.0907$ fm. Five values of the (degenerate) up and down quark masses are considered, with hopping parameter values of $\kappa_{ud} = 0.13700, 0.13727, 0.13754, 0.13770$ and 0.13781; for the strange quark $\kappa_s = 0.13640$. We consider 350 configurations for the four heavier quarks, and 198 configurations for the lightest quark. An ensemble of 750 samples for the lightest quark mass is created by using multiple fermion sources on each configuration, spaced to sample approximately independent regimes of each configuration. Our error analysis is performed using a second-order jackknife method, where the χ^2/dof for projected correlator fits is obtained via a covariance matrix analysis. Our fitting method is discussed in Refs. [25, 27].

The nucleon interpolator we use is the local scalar-diquark interpolator, which provides good overlap with the Roper state in quenched QCD [27]. In constructing our correlation matrices, we consider an extensive sample of different levels of gauge-invariant Gaussian smearing [31] at the fermion source and sink, including 4, 9, 16, 25, 35, 50, 70, 100, 125, 200, 400, 800 and 1600 sweeps. These levels of smearing correspond to rms radii in lattice units ($a \simeq 0.09$ fm) of 1.20, 1.79, 2.37, 2.96, 3.50, 4.19, 4.95, 5.920, 6.63, 8.55, 12.67, 15.47 and 16.00.

Fig. 1 displays effective mass plots, $m(t) = \ln\{G^{+}_{ij}(t)/G^{+}_{ij}(t+1)\}$ for smeared-source to point-sink correlators. The variation in the superposition of excited state contributions is revealed in the different approaches of the effective mass to the ground state plateau where the results converge. From these plots, it is clear that the correlation matrix analysis for excited state contributions will be most effective in the regime $t = 17 - 21$.

To explore the low-lying eigenstates of the nucleon spectrum, we construct several 4×4 correlation matrices as described in Table I. These matrices provide robust results for the lowest three energy eigenstates, with

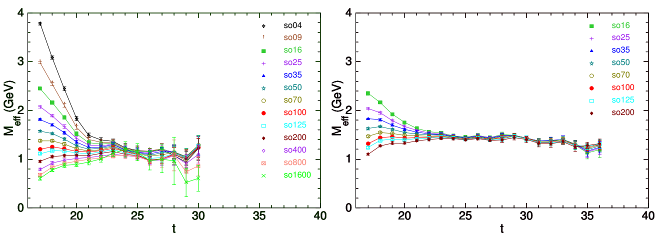

FIG. 1: (Color online). Effective mass from smeared-source to point-sink correlators for various levels of smearings at the source for $\kappa_{ud} = 0.13770$ (left) and $\kappa_{ud} = 0.13700$ (right).

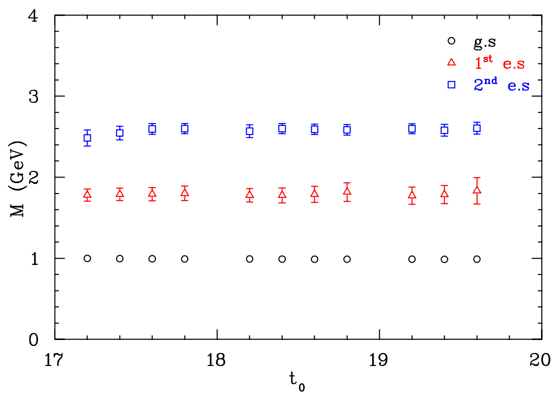

FIG. 2: (Color online). Masses from the projected correlation functions as shown in Eq. 7, for each set of variational parameters t_0 (major axis) and $\triangle t$ (minor axis). This figure corresponds to the lightest quark mass, $\kappa_{ud} = 0.13781$, and the 3rd basis of Table I.

the highest energy level accommodating the fourth eigenenergy and any residual strength from higher states not eliminated via Euclidean time evolution.

The masses from the projected correlation functions obtained from the correlation matrix analysis are very consistent over the variational parameters (t_0,$\triangle t$) as illustrated in Fig. 2. Careful examination of Fig. 2 reveals some systematic drift in the second excited state mass at small $\triangle t$ for $t_0 = 17, 18$. This emphasises the preference for selecting larger values of (t_0,$\triangle t$) as discussed in Refs. [26, 27, 29]. However, larger uncertainties are evident for $t_0 = 18, 19$ with large $\triangle t$ due to the suppression of excited states via Euclidean time evolution. We select t_0=18, $\triangle t$=2 as providing the best balance between these systematic and statistical uncertainties. These variational parameters also provide a projected correlation function having the most favorable χ^2/dof in the effective mass fit.

TABLE I: Smearing levels used in constructing 4×4 correlation matrix bases.

Sweeps →	16	25	35	50	70	100	125	200	400	800
Basis No. ↓	Bases									
1	16	-	35	-	70	100	-	-	-	-
2	16	-	35	-	70	-	125	-	-	-
3	16	-	35	-	-	100	-	200	-	-
4	16	-	35	-	-	100	-	-	400	-
5	16	-	-	50	-	100	125	-	-	-
6	16	-	-	50	-	100	-	200	-	-
7	16	-	-	50	-	-	125	-	-	800
8	-	25	-	50	-	100	-	200	-	-
9	-	25	-	50	-	100	-	-	400	-
10	-	-	35	-	70	-	125	-	400	-

The consistency of the extracted masses from all the 4×4 matrices considered in Table I is illustrated in Fig. 3. In particular, the ground and Roper states are robust. Both lower and higher smearing radii are beneficial for spanning the space of states at all quark mass. However, we avoid bases which include extreme smearing counts (400 and 800) as these often provide ill-defined correlation matrices. Hence, we select basis number 3 as the focus of subsequent analysis.

In Fig. 4, masses of the low-lying positive-parity states of the nucleon are presented with the scale set via the Sommer parameter [32]. The most significant result of this investigation is the manner in which the extracted Roper state (filled triangles) approaches the physical value. The significant curvature in the chiral regime indicates the important role played by mesonic dressings of the Roper. Remaining discrepancies can be attributed to finite volume effects [33]. The strength of the pion-induced self energy revealed here hints at strong mixings of the Roper not only with the ground state nucleon but also with other nearby positive parity states.

The other significant finding of this investigation is the absence of the low-lying multi-particle scattering states at light quark mass. This is most likely attributed to poor overlap between these scattering states and the three-quark interpolating fields used herein. Future calculations should investigate the use of five-quark operators to ensure better overlap with these states. Indeed, complete knowledge of the spectrum is required for a definitive determination of the properties of the Roper resonance.

Fig. 5 provides a comparison of our results in full QCD with earlier results in quenched QCD [26], where the effects of dynamical quark loops are not considered. While the ground state of the nucleon in quenched (open symbols) and full QCD (full symbols) are in reasonable agree-

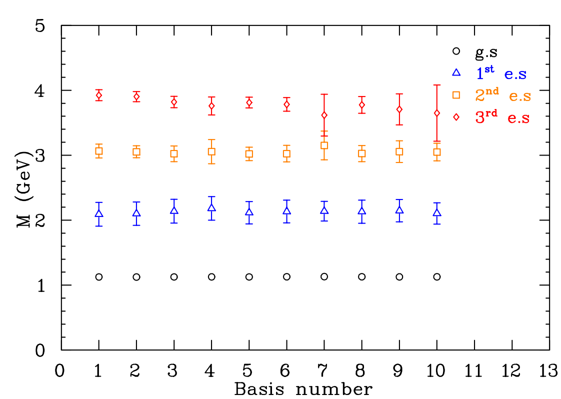

FIG. 3: (Color online). Masses of the $N\frac{1}{2}^+$ energy states for various 4×4 correlation matrix bases as given in Table I, for $\kappa_{ud} = 0.13770$, over 50 configurations.

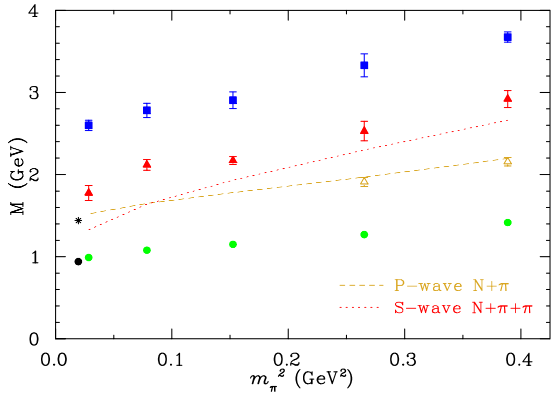

FIG. 4: (Color online). Masses of the low-lying positive-parity states of the nucleon. Physical values are plotted at the far left. Lattice results for the Roper (filled triangles) reveal significant chiral curvature towards the physical mass.

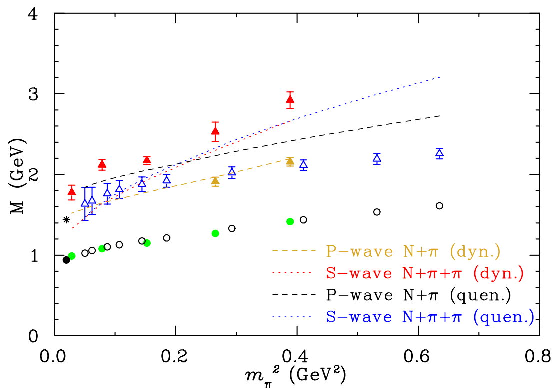

FIG. 5: (Color online). A comparison of the low-lying positive-parity spectrum of dynamical QCD (full symbols) and quenched QCD results (open symbols) from Ref. [26].

ment, significant differences are observed for the Roper in the light quark mass regime. Once again, this emphasizes the role of dynamical fermion loops in creating the mesonic dressings of the Roper.

This investigation is the first to illustrate the manner in which the Roper resonance of Nature manifests itself in today's best numerical simulations of QCD. The quark mass dependence of the state revealed herein substantiates the essential role of dynamical fermions and their associated non-trivial light-mesonic dressings of baryons, which give rise to significant chiral non-analytic curvature in the Roper mass in the chiral regime.

This research was undertaken on the NCI National Facility in Canberra, Australia, which is supported by the Australian Commonwealth Government. We also acknowledge eResearch SA for generous grants of supercomputing time. This research is supported by the Australian Research Council.

[1] L. D. Roper, Phys. Rev. Lett., **12**, 340 (1964).
[2] N. Isgur and G. Karl, Phys. Lett., **B72**, 109 (1977).
[3] N. Isgur and G. Karl, Phys. Rev., **D19**, 2653 (1979).
[4] Z.-p. Li, V. Burkert, and Z.-j. Li, Phys. Rev., **D46**, 70 (1992).
[5] C. E. Carlson and N. C. Mukhopadhyay, Phys. Rev. Lett., **67**, 3745 (1991).
[6] P. A. M. Guichon, Phys. Lett., **B164**, 361 (1985).
[7] O. Krehl, C. Hanhart, S. Krewald, and J. Speth, Phys. Rev., **C62**, 025207 (2000), arXiv:nucl-th/9911080 .
[8] S. Aoki *et al.* (PACS-CS), Phys. Rev. D, **79**, 034503 (2009), arXiv:0807.1661 [hep-lat] .
[9] S. Durr *et al.*, Science, **322**, 1224 (2008), arXiv:0906.3599 [hep-lat] .
[10] D. B. Leinweber, Phys. Rev., **D51**, 6383 (1995), nucl-th/9406001 .
[11] F. X. Lee and D. B. Leinweber, Nucl. Phys. Proc. Suppl., **73**, 258 (1999), arXiv:hep-lat/9809095 .
[12] M. Gockeler *et al.* (QCDSF), Phys. Lett., **B532**, 63 (2002), arXiv:hep-lat/0106022 .
[13] S. Sasaki, T. Blum, and S. Ohta, Phys. Rev., **D65**, 074503 (2002), hep-lat/0102010 .
[14] W. Melnitchouk *et al.*, Phys. Rev., **D67**, 114506 (2003), hep-lat/0202022 .
[15] F. X. Lee *et al.*, Nucl. Phys. Proc. Suppl., **119**, 296 (2003), hep-lat/0208070 .
[16] R. G. Edwards, U. M. Heller, and D. G. Richards (LHP), Nucl. Phys. Proc. Suppl., **119**, 305 (2003), arXiv:hep-lat/0303004 .
[17] N. Mathur *et al.*, Phys. Lett., **B605**, 137 (2005), hep-ph/0306199 .
[18] S. Sasaki, Prog. Theor. Phys. Suppl., **151**, 143 (2003), arXiv:nucl-th/0305014 .
[19] S. Basak *et al.*, Phys. Rev., **D76**, 074504 (2007), arXiv:0709.0008 [hep-lat] .
[20] J. M. Bulava *et al.*, Phys. Rev., **D79**, 034505 (2009), arXiv:0901.0027 [hep-lat] .
[21] J. Bulava *et al.*, Phys. Rev., **D82**, 014507 (2010), arXiv:1004.5072 [hep-lat] .
[22] G. P. Engel, C. B. Lang, M. Limmer, D. Mohler, and A. Schafer (BGR [Bern-Graz-Regensburg]), Phys. Rev., **D82**, 034505 (2010), arXiv:1005.1748 [hep-lat] .
[23] C. Michael, Nucl. Phys., **B259**, 58 (1985).
[24] M. Luscher and U. Wolff, Nucl. Phys., **B339**, 222 (1990).
[25] M. S. Mahbub *et al.*, Phys. Rev., **D80**, 054507 (2009), arXiv:0905.3616 [hep-lat] .
[26] M. S. Mahbub *et al.*, Phys. Lett., **B679**, 418 (2009), arXiv:0906.5433 [hep-lat] .
[27] M. S. Mahbub, A. O. Cais, W. Kamleh, D. B. Leinweber, and A. G. Williams, Phys. Rev., **D82**, 094504 (2010), arXiv:1004.5455 [hep-lat] .
[28] M. S. Mahbub, W. Kamleh, D. B. Leinweber, A. O. Cais, and A. G. Williams, Phys. Lett., **B693**, 351 (2010), arXiv:1007.4871 [hep-lat] .
[29] B. Blossier, M. Della Morte, G. von Hippel, T. Mendes, and R. Sommer, JHEP, **04**, 094 (2009), arXiv:0902.1265 [hep-lat] .
[30] Y. Iwasaki, UTHEP-118.
[31] S. Gusken, Nucl. Phys. Proc. Suppl., **17**, 361 (1990).
[32] R. Sommer, Nucl. Phys., **B411**, 839 (1994), arXiv:hep-lat/9310022 .
[33] R. D. Young, D. B. Leinweber, A. W. Thomas, and S. V. Wright, Phys. Rev., **D66**, 094507 (2002), arXiv:hep-lat/0205017 .